Clinical research

Double heterozygous variants in *FBN1* and *FBN2* in a Thai woman with Marfan and Beals syndromes

Chureerat Phokaew[a,b,c], Rekwan Sittiwangkul[d], Kanya Suphapeetiporn[a,c,*], Vorasuk Shotelersuk[a,b,c]

[a] *Center of Excellence for Medical Genomics, Medical Genomics Cluster, Department of Pediatrics, Faculty of Medicine, Chulalongkorn University, Bangkok, Thailand*
[b] *Research Affairs, Faculty of Medicine, Chulalongkorn University, Bangkok, 10330, Thailand*
[c] *Excellence Center for Genomics and Precision Medicine, King Chulalongkorn Memorial Hospital, the Thai Red Cross Society, Bangkok, 10330, Thailand*
[d] *Department of Pediatrics, Faculty of Medicine, Chiang Mai University, 50200, Chiang Mai, Thailand*

A B S T R A C T

A phenotype of an individual is resulted from an interaction among variants in several genes. Advanced molecular technologies allow us to identify more patients with mutations in more than one genes. Here, we studied a Thai woman with combined clinical features of Marfan (MFS) and Beals (BS) syndromes including frontal bossing, enophthalmos, myopia, the crumpled appearance to the top of the pinnae, midface hypoplasia, high arched palate, dermal stretch marks, aortic enlargement, mitral valve prolapse and regurgitation, aortic root dilatation, and progressive scoliosis. The aortic root enlargement was progressive to a diameter of 7.2 cm requiring an aortic root replacement at the age of 8 years. At her last visit when she was 19 years old, she had moderate aortic regurgitation. Exome sequencing revealed that she carried the c.3159C > G (p.Cys1053Trp) in exon 26 of *FBN1* and c.2638G > A (p. Gly880Ser) in exon 20 of *FBN2*. The variant in *FBN1* was *de novo*, while that in *FBN2* was inherited from her unaffected mother. Both genes encode for fibrillins, which are essential for elastic fibers and can form the heterotypic microfibrils. Two defective fibrillins may synergistically worsen cardiovascular manifestations seen in our patient. In this study, we identified the fourth patient with both MFS and BS, carrying mutations in both *FBN1* and *FBN2*.

1. Introduction

Marfan syndrome (MFS) is an autosomal dominant connective tissue disorder affecting cardiovascular, skeletal, and ocular systems. Its estimated prevalence is at 1/5000–1/10,000. MFS is caused by mutations in *FBN1* (Dietz, 1993). Congenital contractural arachnodactyly (CCA) or Beals Syndrome (BS), is an autosomal dominant disorder, characterized by crumpled ears, craniofacial abnormalities including frontal bossing, a progressive scoliosis, joint contractures, adducted thumbs, and long, thin and flexed digits. Its prevalence is unknown but appears to be lower than that of MFS. BS is caused by mutations in *FBN2* (Godfrey, 1993).

Since MFS and BS affect similar tissues including those in the cardiovascular system, mutations in both *FBN1* and *FBN2* may synergistically worsen clinical manifestations and disease progression. An abortus was found to harbor variants in both *FBN1* and *FBN2*. Here, we report a 19-year-old woman having combined clinical features of MFS and BS. Whole exome sequencing identified double heterozygous variants in *FBN1* and *FBN2*. To our knowledge, she is the fourth patient with both MFS and BS.

2. Materials and methods

The study was approved by the institutional review board (IRB) of the Faculty of Medicine, Chulalongkorn University, Thailand (IRB # 706/62). After informed consent, blood samples from the proband and her parents were collected. The trio whole exome sequencing analysis was performed and gene prioritization was done using Exomiser (Supplementary method). Sanger sequencing was used to confirm the existence of the variants in the trio. ClustalW embedded in UGENE (Okonechnikov et al., 2012) was used to study protein evolutionary conservation. Protein 3D structure was constructed by the automated protein-homology modeling server SWISS-MODEL and validated with the PyMOL software (Supplementary method).

---

* Corresponding author. Division of Medical Genetics and Metabolism, Department of Pediatrics, Faculty of Medicine, Chulalongkorn University, Sor Kor Building 11th floor, Bangkok, 10330, Thailand.
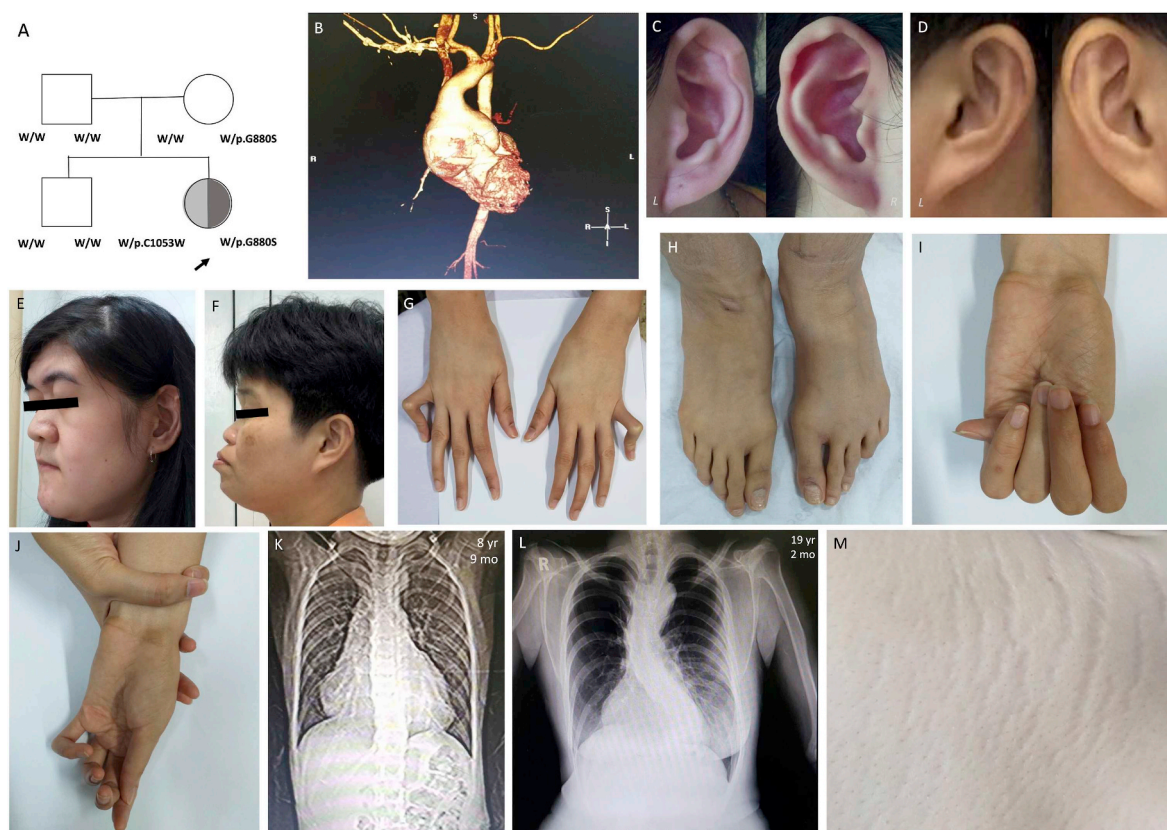*E-mail address:* kanya.su@chula.ac.th (K. Suphapeetiporn).

Fig. 1. The pedigree, clinical, radiographic and cardiovascular CT scan of the proband and her unaffected mother. The proband is the only affected member in the pedigree (A), crumpled ears present in the proband (C) but absent in her mother (D), arachnodactyly (G, H, I, J), mild scoliosis at 8 yr 9 mo (K), and 19 yr 2 mo (L), stretch marks (M), the aortic root dilatation 7.2 cm before her surgery at age 8 yr 9 mo (B), and frontal bossing in the proband (E) but absent in her mother (F).

3. Results

3.1. Clinical report

The proband was born at term with birth weight of 3.1 kg (25th centile). She was first referred to the Maharaj Nakorn Chiang Mai Hospital at the age of 1 year 11 months for an evaluation of dysmorphic features. Her weight was 9.5 kg (10th centile) and height 90 cm (90th centile). She had frontal bossing, high arched palate, crumbled ears, pectus carinatum, dolichostenomelia, arachnodactyly of fingers and toes, camptodactyly of fifth fingers, leg length discrepancy, and a grade III/VI systolic murmur at the cardiac apex. The arm span to height ratio was 1.01 (91/90 cm). Echocardiography revealed a mitral valve prolapse with moderate mitral regurgitation, a bicuspid aortic valve, and a severe aortic root dilatation with a diameter of 3.76 cm (Z-score of +15, www.marfan.org). She was diagnosed with MFS and consequently given propranolol 1 mg/kg/day and enalapril 0.1 mg/kg/day. The leg length discrepancy was found to be caused by a left hip dislocation which was treated by a closed reduction and a hip spica cast. She was the second child with one healthy older brother (Fig. 1A). The parents were healthy without clinical features of MFS or BS.

At the age of five years, she developed myopia without lens dislocation. Notably, even with the medications, the follow-up echocardiograms showed progressive mitral valve prolapse, mitral valve regurgitation and aortic root dilatation as shown in Table 1. When she was 8 years and 9 months, the computed tomographic angiography (CTA) of the aorta showed aortic root diameter of 7.2 cm (Z-score +27) (Fig. 1B) requiring cardiovascular surgery with aortic-valve-sparing aortic-root replacement (David technique) and concomitant mitral valve repair. At the age of 18 years, the follow up CTA of the aorta showed additional dilatation of the ascending aorta from the distal part

to the aortic-root graft and the entire aortic arch. The CTA imaging also revealed dural ectasia and lateral meningocele at the lumbosacral region. At her last visit at 19 years old, her weight was 45.5 kg (37th centile), height 156.5 cm (37th centile), and blood pressure 108/66 mmHg. Her arm span was 162 cm while her height was 156.5 cm. Her upper segment to lower segment ratio was 0.8 (69.5 cm: 87 cm), supporting the dolichostenomelia feature. She had crumpled ears (Fig. 1C), midface hypoplasia (Fig. 1E), prognathia, no audible heart murmur, arachnodactyly of fingers and toes, flexion deformities of toes (Fig. 1G and H), camptodactyly of fifth fingers (Fig. 1G), positive thumb and wrist signs (Fig. 1I and J), severe thoraco-lumbar scoliosis (Fig. 1K and L) and many stretch marks on her skin (Fig. 1M). Echocardiography revealed moderate aortic regurgitation, moderate tricuspid valve prolapse with moderate tricuspid regurgitation, and borderline decreased left ventricular systolic function.

3.2. Variant identification and bioinformatic analysis

Whole exome sequencing of the proband revealed two heterozygous missense mutations. The first is a c.3159C > G (p.Cys1053Trp) in exon 26 of *FBN1* (NM_000138). The p.Cys1053Trp mutation has never been previously reported in patients with MFS. It is not in the GnomAD (biorxiv = 531210v2) or dbSNP databases and predicted to be deleterious by SIFT (score = 0.000) and PolyPhen-2 (score = 0.998). PCR-Sanger sequencing confirmed the presence of the mutation in the proband and showed that both parents harbored only the wild-type allele, indicating that the p.Cys1053Trp mutation in *FBN1* in the proband is *de novo* (Fig. 2A). The p.Cys1053Trp variant in *FBN1* occurs in the cbEGF-like domain at one of the six critical Cys residues.

The other mutation is a c.2638G > A (p. Gly880Ser) in exon 20 of *FBN2* (NM_001999). The p.Gly880Ser has never been previously

Table 1
Clinical features of the current case and others harboring sequence variants in *FBN1* and *FBN2*.

Clinical phenotype	Marfan syndrome	Beals syndrome	Neonatal Marfan syndrome	Severe Beals syndrome	Current case	Aggarwal S (Aggarwal et al., 2018)	Case Ab2 (Najafi et al., 2020)	Case Ab4 (Najafi et al., 2020)	Case Ac1 (Najafi et al., 2020)
Age at examination (year/sex)					1 y 11 months/F	29-week fetus/NA	12 y/F	45 y/M	21 y/M
Eye problems	Y (severe nearsightedness, dislocated lens, detached retina, early glaucoma, and early cataracts)	Y	Y		Y (myopia)				Y (myopia)
Deep-set eyes (enophthalmos)	Y				Y				
Downward slanting of the eyes	Y		Y						
Abnormalities affecting the head and face (craniofacial)		Y							
Crumpled appearance to the top of the ears		Y	Y	Y	Y	Y		Y	
Frontal bossing		Y			Y				
3 of 5 facial features	Y		Y		Y				Y
Dolichocephaly or scaphocephaly		Y							
Brachycephaly		Y							
Midface hypoplasia	Y				Y				
Dolichocephaly	Y								
Crowded teeth	Y								
An abnormally short neck		Y							
High-arched palate	Y	Y			Y		Y		
Micrognathia	Y	Y							
Aortic enlargement and aortic root dilatation	Y	Y	Y		Y				Y
Mitral regurgitation	Y	Y							
Aortic dilation (cm)					+ (7.2) (Z-score > 2.0)			+ (4.9) (Z-score > 2.0)	+ (4.1) (Z-score > 2.0)
Mitral valve prolapse	Y	Y	Y		Y				
Tricuspid valve prolapse	Y		Y		Y				
Arrhythmias	Y								
Atrial or ventricular septal defect				Y					
Single umbilical artery				Y					
Interrupted aortic arch		Y		Y					
Enlargement of the proximal pulmonary artery	Y								
Duodenal or esophageal atresia				Y					
Pectus carinatum & excavatum	Y	Y			Y (carinatum)		Y (excavatum)	Y (carinatum & excavatum)	Y (carinatum)
Increased total and residual lung volume	Y								
Pulmonary emphysema			Y	Y					
Retrognathia	Y								
Backward or lateral curved spine at birth or early childhood		Y		Y	Y				
Progressive scoliosis	Y	Y			Y		Y		
Reduced bone mass		Y							
An abnormally deep hip socket (acetabulum)	Y	–			Y (bilateral hip dislocation)	Y (bilateral hip dislocation)			
Curved spine	Y	Y		Y	Y				Y
Intestinal malrotation				Y					
Gastrointestinal anomalies				Y	Y	Y			

Table 1 (*continued*)

Clinical phenotype	Marfan syndrome	Beals syndrome	Neonatal Marfan syndrome	Severe Beals syndrome	Current case	Aggarwal S (Aggarwal et al., 2018)	Case Ab2 (Najafi et al., 2020)	Case Ab4 (Najafi et al., 2020)	Case Ac1 (Najafi et al., 2020)
Contractures (fingers, elbows, knees, toes, and hips)		Y		Y	Y		Y	Y	
Long arms, legs and fingers	Y	Y		Y	Y				
Tall and thin body type	Y	Y			Y				
Wrist sign	Y	Y			Y		Y	Y	Y
Thumb sign	Y	Y			Y		Y	Y	Y
Flexible joints	Y								
Reduced elbow extension (r/l)					+/+		+/+	+/+	> 180°/ > 180°
Dolichostenomelia US/LS ratio < 0.85 (height, cm)					+ (156.5)		- (159)	+ (179.5)	- (188)
Arm span/height ratio > 1.05 (arm span, cm)					- (162)		- (159)	- (188.5)	+ (205)
Ghent nosology systemic score					>7		7	>7	>7
Muscular hypoplasia		Y		Y					
Joint deformity		Y							
Limb joint contracture		Y							
Congenital contracture		Y		Y		Y			
Striae distensae	Y				Y				
Pes planus	Y				Y		Y	Y	Y
Mutation	Various	FBN2 exons 24-34	FBN1 exons 24–27 & exons 31, 32	FBN2 exons 24-36	FBN1 exon 26, FBN2 exon 20	FBN1 exon 49, FBN2 exon 23	FBN1 exon 66, FBN2 introns 30-31	FBN1 exon 66, FBN2 intron 30-31	FBN1 exon 54, FBN2 exon 27

reported in patients with BS. It is found in five of 251,376 alleles (two East Asians, one African and two non-Finnish Europeans) in the GnomAD database (biorxiv = 531210v2) without any homozygous subjects, present in dbSNP (rs555682061), and predicted to be deleterious by SIFT (score = 0.009) and PolyPhen-2 (score = 1). Interestingly, p.Gly880Asp is also in gnomAD (5/113710 non-Finnish Europeans). PCR-Sanger sequencing confirmed the presence of the mutation in the proband and showed that her mother also harbored the mutation (Fig. 2A).

Both mutations were absent in our in-house 1690 unrelated Thai exome database. Both altered amino acid positions are highly conserved among species, from frogs to humans (Fig. 2B). ClinVar accession numbers of c.3159C > G (p.Cys1053Trp) and c.2638G > A (p.Gly880Ser) are SCV001222473 and SCV001222474, respectively.

### 3.3. In silico protein structure analysis

FBN1 and *FBN2* have similar gene structures (Fig. 2C). According to the 271 aa 3D protein structure comparison, the fibrillin 1 with Trp1053 3D structure is different from that with Cys1053 (Fig. 2D). The wild-type Cys1053 forms a disulfide bond with Cys1039 (Fig. 2E), but the bond disappears with the mutant Trp1053 (Fig. 2F).

The 3D structures of the fibrillin 2 with Ser880 and Gly880 are different (Fig. 2G). The mutant Ser880 (Fig. 2I) generates a new H-bond between Ser880 and Leu883 which does not exist with the wild-type Gly880 (Fig. 2H).

4. Discussion

We report a Thai woman with combined features of Marfan (MFS) and Beals (BS) syndromes (Table 1). Her features specific to MFS include enophthalmos, midface hypoplasia, and the stretch marks on the skin that are not related to weight gain or loss. Her BS specific phenotypes include the crumpled appearance to the top of the pinnae and frontal bossing. She also had features present in both syndromes including myopia, high arched palate, aortic enlargement, mitral regurgitation, mitral valve prolapse, aortic root dilatation, and progressive scoliosis. Notably, the proband's mother who also harbored the *FBN2* variant did not have crumpled ears (Fig. 1D) nor frontal bossing (Fig. 1F). Echocardiography revealed normal cardiac structure and function.

Using whole exome sequencing, she was found to harbor heterozygous variants in *FBN1* and *FBN2*, the genes causing MFS and BS, respectively. The p.Cys1053Trp mutation in *FBN1* is *de novo* and has never been previous reported. The amino acid residue Cys1053 forms the 50th disulfide bond with the residue Cys1039 of fibrillin-1. The disruption of the 50th disulfide bond of fibrillin-1 in a mouse model led to progressive deterioration of aortic wall and skeletal deformation (Judge et al., 2004) supporting the pathogenicity of the p.Cys1053Trp in humans. Notably, other mutations involving the wild-type p.Cys1053 in *FBN1* have previously been reported (http://www.ncbi.nlm.nih.gov/clinvar and (Putnam et al., 1996)). These include p.Cys1053Arg (NM_00138.4 (*FBN1*):c.3157T > C, p.Cys1053Ser (NM_000138.4(*FBN1*):c.3157T > A, variant id 549135), p.Cys1053Gly (NM_000138.4(*FBN1*):c.3157T > G, variant id 547307) and p.Cys1053Ter (NM_000138.4(*FBN1*):c.3159C > A, variant id 264131), respectively. The patient with p.Cys1053Ter was born with congenital contracture, scoliosis, and arachnodactyly. She was diagnosed with a severe neonatal MFS (nMFS). At the age of 1 year and 10 months, she had failure to thrive due to progressive heart failure, dilatation of the sinuses of Valsalva, mitral valve regurgitation and worsening cardiac contractility, and later died postoperatively (Putnam et al., 1996). The phenotype of the other patient with p.Cys1053Arg reported by Putnam et al. (1996) included cardiovascular complications (mitral valve regurgitation, aortic valve incompetence), congenital contracture, abnormal face (frontal bossing and deep-set eyes), abnormal ears, and
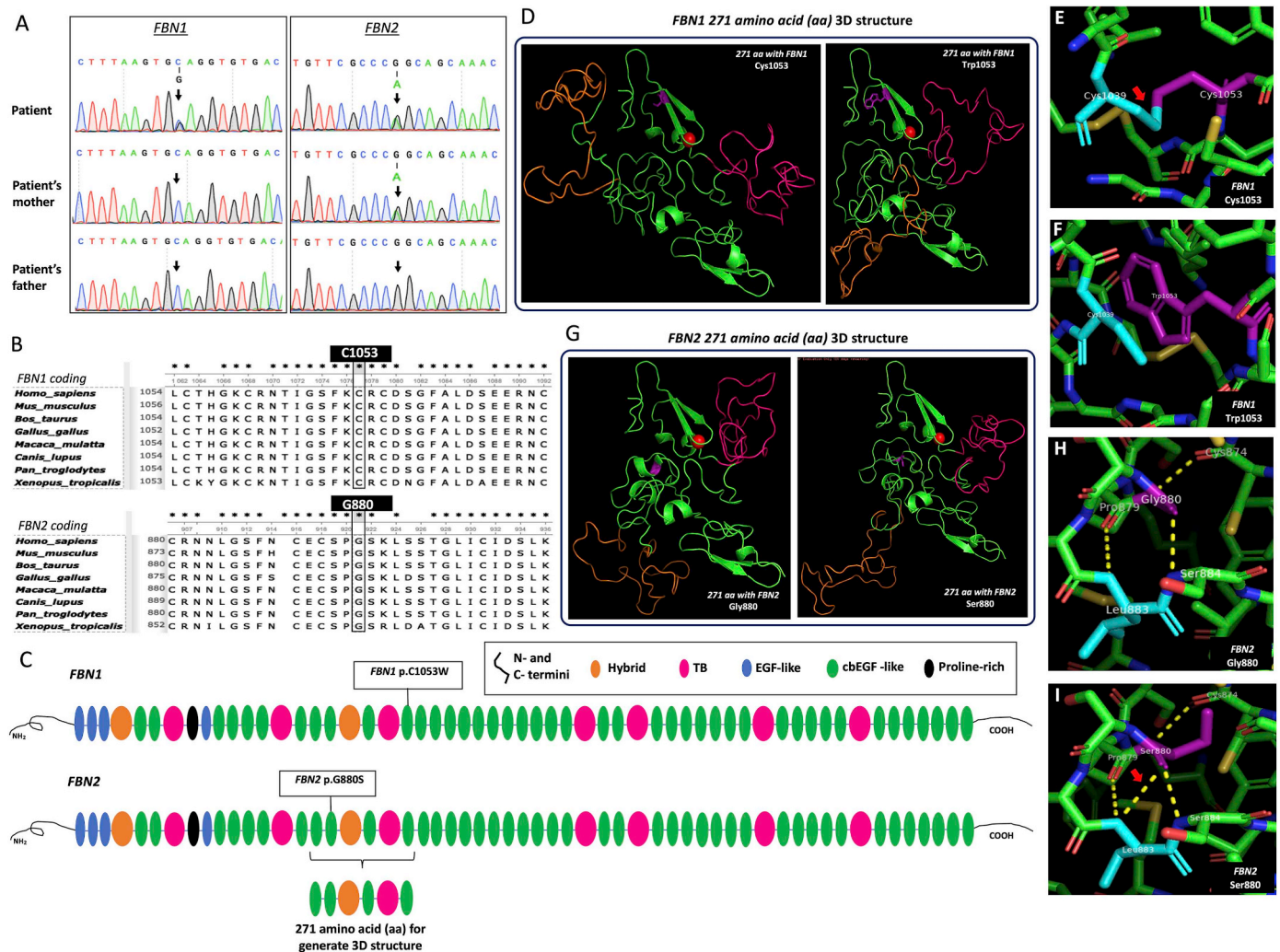
Fig. 2. The molecular finding and predicted 3D protein changes. Sanger sequencing shows that she harbors the *de novo FBN1* mutation, p.Cys1053Trp, and the p.Gly880Ser mutation in *FBN2* which was inherited from her unaffected mother (A). Both amino acid residues are evolutionarily conserved from frogs to humans (B). The structures of FBN1 and FBN2 with the mutated amino acids (C). The 3D structure of the 271 amino acids containing the p.Cys1053Trp (D) and p.Gly880Ser (G). The structural prediction shows changes of overall structural patterns; the purple amino acids indicate mutant amino acids. The wild-type Cys1053 forms the 50th disulfide bond (an arrow) with Cys1039 (E); with the mutant Trp1053, the disulfide bond disappears (F). The wild-type Gly880 does not form a hydrogen bond with Leu883 (H), while the mutant Ser880 forms a hydrogen bond with Leu883 (an arrow) (I). (For interpretation of the references to colour in this figure legend, the reader is referred to the Web version of this article.)

failure to thrive due to progressive heart failure.

Several lines of evidence suggest that the p.Gly880Ser in *FBN2* is pathogenic. The nonpolar glycine at the amino acid residue 880 is evolutionarily conserved and its change to the polar serine is predicted to be deleterious by SIFT and PolyPhen-2. The Gly880 is conserved within the cbEGF-like domain number 13. The predicted 3D structure of the fibrillin-2 with the wild-type Gly880 shows no polar bond with Leu883, while the mutant Ser880 induces a hydrogen bond between Ser880 and Leu883. This may change the overall 3D structure of fibrillin-2 (Fig. 2G) and influence the protein conformation leading to its pathogenicity (You et al., 2017).

The 'neonatal regions', referring to the genetic regions of *FBN1* and *FBN2* of which mutations lead to nMFS and severe BS, respectively, are exons 24–32 of *FBN1* (Le Gloan et al., 2016) and exons 24–36 of *FBN2* (Godfrey, 1993). The p.Cys1053Trp in *FBN1* found in our patient is located in exon 26 within the neonatal region of *FBN1*. It encodes for the highly conserved calcium binding consensus sequence of cbEGF-like domain number 15. The mutation occurs at one of the six critical Cys residues of this domain. Alterations of amino acids within the cbEGF domain change calcium binding properties of fibrillin-1 and interfere

with stabilization of the microfibril architecture within connective tissues of MFS (Handford, 2000). Nonetheless, mutations in 'neonatal regions' of *FBN1* do not always lead to nMFS; several patients with mutations in this region have classic MFS (Loeys et al., 2001). In fact, mutations in exon 26 of *FBN1* have previously been reported in patients with classic MFS (Arbustini et al., 2005; Loeys et al., 2001). On the other hand, several cases of nMFS have mutations outside the 'neonatal regions (Le Gloan et al., 2016; Loeys et al., 2001).

Since our proband's mother who carries the *FBN2* variant does not have features of BS, the p.Gly880Ser variant in *FBN2* may be non-penetrant (Arbustini et al., 2005; Loeys et al., 2001) in the mother but contribute to the anomalies in the proband. There were reports of non-penetrants in individuals who were mosaic for mutations in *FBN2* (Putnam et al., 1997; Wang et al., 1996). Nonetheless, it remains possible that the *FBN2* variant is not pathogenic and all features seen in the proband are solely resulted from the mutation in *FBN1*. In our view, the clinical features of our patient are more consistent with a diagnosis of both MFS and BS, caused by the double heterozygous mutations in both *FBN1* and *FBN2*. Whole-exome sequencing allows us to provide multi-locus diagnoses (Posey et al., 2017)' (Porntaveetus et al., 2017). Among

cases of digenic inheritance, 37.5% (30 from 80 digenic cases) have overlapping phenotypic features (Posey et al., 2017). Mutations in both genes may act synergistically leading to a more severe manifestation. The fibrillin-1 and fibrillin-2 are two highly similar fibrillins, cysteine-rich glycoproteins, essential for the elastic fiber formation within connective tissues allowing many tissues in the body to resume their shape after contracting or stretching. Both fibrillins are absolutely essential for vascular development (Carta et al., 2006; Chaudhry et al., 2001). There is evidence that fibrillin-1 and fibrillin-2 can form the heterotypic fibrillin-1/fibrillin-2 microfibrils (Lin et al., 2002). The defective fibrillin-1 and fibrillin-2 may enhance the abnormality of microfibril formation and explain the severity of the proband who at the age of 7 years had the aortic sinus diameter of 7.2 cm (mean of those of healthy at age 9 years: 2.07 cm; Marfan Z-score = 27.06) (Kaiser et al., 2008). Even compared with children with the classic MFS whose aortic root diameters range from 1.7 to 4.6 cm (mean 3.154 ± 0.650 cm) (Wozniak-Mielczarek et al., 2019), the aortic root of our proband was significantly more dilated.

An abortus was previously reported to harbor variants in these two genes. It carried the c.6004C > T (p.Pro2002Ser) in exon 49 of *FBN1* (NM_000138.4) and the c.2945G > T (p.Cys982Phe) in exon 23 of *FBN2* (NM_001999.3). At 29-week gestation, the fetus was found to have multiple severe phenotypes and terminated (Aggarwal et al., 2018). In addition, three members from two families were recently reported to carry variants in two genes; the first family harbored the c.8489A > G (p.Gln2830Arg) in exon 66 of *FBN1* and the c.3974-26T > G (p.Asn1327_Val1368del) in introns 30–31 of *FBN2* while the second family carried the c.6595G > A (p.Gly2199Ser) in exon 54 of *FBN1* and the c.3481G > A (p. Glu1161Lys) in exon 27 of *FBN2* (Najafi et al., 2020). Our patient is the fourth living individual with both MFS and BS, having mutations in both *FBN1* and *FBN2*. The mutations in these two genes lead to defects in both fibrillins, which may synergistically worsen cardiovascular manifestations in the patient.

CRediT authorship contribution statement

Chureerat Phokaew: Formal analysis, Visualization, Writing - original draft, Writing - review & editing. **Rekwan Sittiwangkul:** Investigation, Formal analysis, Writing - original draft, Writing - review & editing. **Kanya Suphapeetiporn:** Conceptualization, Writing - review & editing, Supervision, Project administration, Funding acquisition. **Vorasuk Shotelersuk:** Conceptualization, Writing - review & editing, Supervision, Project administration, Funding acquisition.

Declaration of competing interest

The authors have no conflicts of interest to disclose.

Appendix A. Supplementary data

Supplementary data to this article can be found online at https://doi.org/10.1016/j.ejmg.2020.103982.

References

Aggarwal, S., Das Bhowmik, A., Tandon, A., et al., 2018. Exome sequencing reveals blended phenotype of double heterozygous FBN1 and FBN2 variants in a fetus. Eur. J. Med. Genet. 61 (7), 399–402.

Arbustini, E., Grasso, M., Ansaldi, S., et al., 2005. Identification of sixty-two novel and twelve known FBN1 mutations in eighty-one unrelated probands with Marfan syndrome and other fibrillinopathies. Hum. Mutat. 26 (5), 494.

Carta, L., Pereira, L., Arteaga-Solis, E., et al., 2006. Fibrillins 1 and 2 perform partially overlapping functions during aortic development. J. Biol. Chem. 281 (12), 8016–8023.

Chaudhry, S.S., Gazzard, J., Baldock, C., et al., 2001. Mutation of the gene encoding fibrillin-2 results in syndactyly in mice. Hum. Mol. Genet. 10 (8), 835–843.

Dietz, H., 1993. Marfan syndrome. In: Adam, M.P., Ardinger, H.H., Pagon, R.A., Wallace, S.E., Bean, L.J.H., Stephens, K., Amemiya, A. (Eds.), GeneReviews((R)). Seattle (WA).

Godfrey, M., 1993. Congenital contractural arachnodactyly. In: Adam, M.P., Ardinger, H.H., Pagon, R.A., Wallace, S.E., Bean, L.J.H., Stephens, K., Amemiya, A. (Eds.), ews ((R)). Seattle (WA). GeneRevi.

Handford, P.A., 2000. Fibrillin-1, a calcium binding protein of extracellular matrix. Biochim. Biophys. Acta 1498 (2–3), 84–90.

Judge, D.P., Biery, N.J., Keene, D.R., et al., 2004. Evidence for a critical contribution of haploinsufficiency in the complex pathogenesis of Marfan syndrome. J. Clin. Invest. 114 (2), 172–181.

Kaiser, T., Kellenberger, C.J., Albisetti, M., et al., 2008. Normal values for aortic diameters in children and adolescents-assessment in vivo by contrast-enhanced CMR-angiography. J. Cardiovasc. Magn. Reson. 10, 56.

Le Gloan, L., Hauet, Q., David, A., et al., 2016. Neonatal marfan syndrome: report of a case with an inherited splicing mutation outside the neonatal domain. Mol Syndromol 6 (6), 281–286.

Lin, G., Tiedemann, K., Vollbrandt, T., et al., 2002. Homo- and heterotypic fibrillin-1 and -2 interactions constitute the basis for the assembly of microfibrils. J. Biol. Chem. 277 (52), 50795–50804.

Loeys, B., Nuytinck, L., Delvaux, I., et al., 2001. Genotype and phenotype analysis of 171 patients referred for molecular study of the fibrillin-1 gene FBN1 because of suspected Marfan syndrome. Arch. Intern. Med. 161 (20), 2447–2454.

Najafi, A., Caspar, S.M., Meienberg, J., et al., 2020. Variant filtering, digenic variants, and other challenges in clinical sequencing: a lesson from fibrillinopathies. Clin. Genet. 97 (2), 235–245.

Okonechnikov, K., Golosova, O., Fursov, M., et al., 2012. Unipro UGENE: a unified bioinformatics toolkit. Bioinformatics 28 (8), 1166–1167.

Porntaveetus, T., Srichomthong, C., Suphapeetiporn, K., et al., 2017. Monoallelic FGFR3 and Biallelic ALPL mutations in a Thai girl with hypochondroplasia and hypophosphatasia. Am. J. Med. Genet. 173 (10), 2747–2752.

Posey, J.E., Harel, T., Liu, P., et al., 2017. Resolution of disease phenotypes resulting from multilocus genomic variation. N. Engl. J. Med. 376 (1), 21–31.

Putnam, E.A., Cho, M., Zinn, A.B., et al., 1996. Delineation of the Marfan phenotype associated with mutations in exons 23-32 of the FBN1 gene. Am. J. Med. Genet. 62 (3), 233–242.

Putnam, E.A., Park, E.S., Aalfs, C.M., et al., 1997. Parental somatic and germ-line mosaicism for a FBN2 mutation and analysis of FBN2 transcript levels in dermal fibroblasts. Am. J. Hum. Genet. 60 (4), 818–827.

Wang, M., Clericuzio, C.L., Godfrey, M., 1996. Familial occurrence of typical and severe lethal congenital contractural arachnodactyly caused by missplicing of exon 34 of fibrillin-2. Am. J. Hum. Genet. 59 (5), 1027–1034.

Wozniak-Mielczarek, L., Sabiniewicz, R., Drezek-Nojowicz, M., et al., 2019. Differences in cardiovascular manifestation of marfan syndrome between children and adults. Pediatr. Cardiol. 40 (2), 393–403.

You, G., Zu, B., Wang, B., Wang, Z., et al., 2017. Exome sequencing identified a novel FBN2 mutation in a Chinese family with congenital contractural arachnodactyly. Int. J. Mol. Sci. 18 (4).